

Human Foamy Virus Replication: A Pathway Distinct from That of Retroviruses and Hepadnaviruses

Shuyuarn F. Yu, David N. Baldwin, Samuel R. Gwynn, Suneetha Yendapalli, Maxine L. Linial*

Human foamy virus (HFV) is the prototype of the *Spumavirus* genus of Retroviridae. In all other retroviruses, the *pol* gene products, including reverse transcriptase, are synthesized as Gag-Pol fusion proteins and are cleaved to functional enzymes during viral budding or release. In contrast, the Pol protein of HFV is translated from a spliced messenger RNA and lacks Gag domains. Infectious HFV particles contain double-stranded DNA similar in size to full-length provirus, suggesting that reverse transcription has taken place in viral particles before new rounds of infection, reminiscent of hepadnaviruses. These data suggest that foamy viruses possess a replication pathway containing features of both retroviruses and hepadnaviruses but distinct from both.

The retroviral replication pathway is understood in great detail, and it has been assumed that all members of the Retroviridae family use the same mechanisms for assembly and reverse transcription (1). The three main types of viruses in this family, onco-, lenti-, and spumaviruses (foamy viruses), have similar genomic structures. They all encode three genes, 5'-*gag-pol-env*-3', that are required for production of infectious particles. The encapsidated genome in all well-characterized retroviruses is a dimer of single-stranded RNA. After infection, reverse transcription produces DNA flanked by long terminal repeats (LTRs) containing important cis-acting elements. Another retroviral hallmark is the presence of a primer binding site located 3' of the 5' LTR for binding of tRNAs, which serve as primers for initiation of reverse transcription, to the genomic RNA. The foamy viruses have not been studied as extensively as the other genera, but given these structural similarities, it was assumed that foamy virus replication followed the retrovirus paradigm. In the onco- and lentiviruses (conventional retroviruses), the *pol* gene products (protease, reverse transcriptase, and integrase) are synthesized as part of a Gag-Pol fusion protein. Gag-Pol is produced from genomic RNA about 5% of the time through one of two mechanisms for translation past a termination signal at the end of *gag*. In some retroviruses this occurs

by -1 ribosomal frameshifting, and in others by use of a suppressor tRNA (2). Pol is assembled into virions by means of the Gag assembly domains on the polyprotein. During viral assembly, protease is activated and Gag and Gag-Pol are cleaved to the mature viral proteins (3). One consequence of this pathway is that activation of reverse transcription occurs only when the protein is encapsidated along with its genomic RNA template. Most reverse transcription occurs after new cells are infected.

Unlike the conventional retroviruses, HFV's largest *pol* gene product is an approximately 125-kD protein that does not contain any Gag protein determinant (4, 5). We therefore considered that another mechanism exists for HFV Pol synthesis. Spliced mRNAs are used for synthesis of Env glycoproteins and nonstructural proteins (such as Bel1 and Bet; Fig. 1A) located at the 3' end of the genome. The only nonstructural protein with a known function is Bel1, which is a transcriptional transactivator (6). All these subgenomic

RNAs use the same 5' splice site (5'ss) located 51 nucleotides from the 5' end of the genomic RNA (7). We investigated the possibility of a spliced *pol* mRNA by using the reverse transcriptase polymerase chain reaction (RT-PCR) to amplify cellular RNA from HFV-infected cells (8). Primers were chosen to produce PCR products including the major 5'ss and part of the protease domain of *pol* (Fig. 1A). These primers should yield a ~2.4-kb product from genomic-length RNA, and a considerably shorter product from a spliced *pol* RNA. Total RNA was extracted from human embryonic lung (HEL) fibroblast cells acutely infected with HFV (9) derived from the molecular clone pHFV13 (10). A RT-PCR product of 0.6 kb was detected from infected but not uninfected cells. DNA from this band was cloned, and the splice site sequenced (Fig. 1B). There is juxtaposition of the major 5'ss and a consensus 3'ss, creating a splice junction at nucleotides 51 and 1848 at the 3' end of the capsid domain of Gag. The AUG at nucleotide 2340 in this RNA is the start of the *pol* open reading frame.

As further confirmation of the existence of a spliced *pol* mRNA, a primer extension assay was developed in which two oligonucleotide primers spanning the *pol* 5'ss and 3'ss (Fig. 2A) were used to produce extension products from a control spliced RNA but not an unspliced RNA (Fig. 2B, lanes 3, 4, 11, and 12). We could detect the spliced *pol* mRNA in HFV-infected cells (lanes 1 and 9). Although this assay is not quantitative, comparison of the intensity of the extension products obtained with primers 4 and 7 (lanes 1 and 9), which are specific for spliced RNA, with that from the unspliced genomic RNA primer 5 (lane 5), suggests that *pol* mRNA is not abundant in infected cells. As a further control, we could not detect any spliced *pol* product using total nucleic acid isolated from virions (11).

To determine whether this putative *pol*

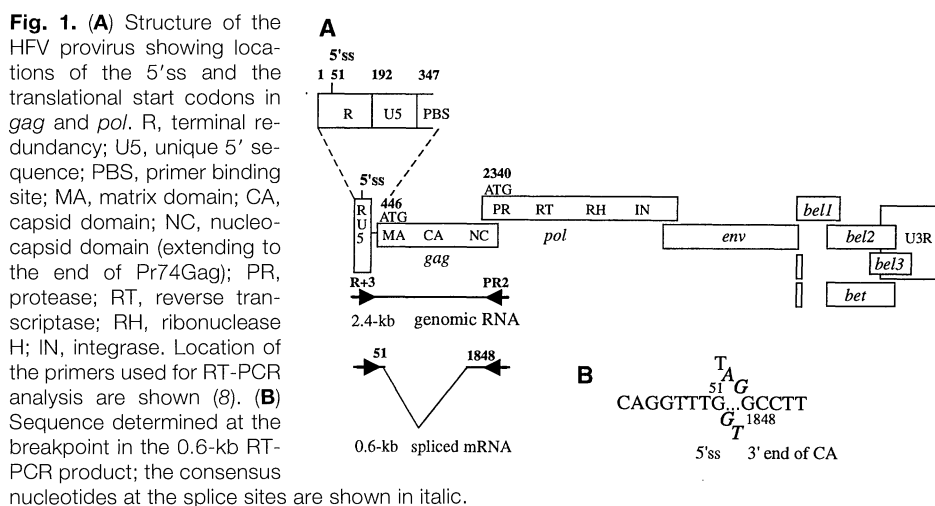


Fig. 1. (A) Structure of the HFV provirus showing locations of the 5'ss and the translational start codons in *gag* and *pol*. R, terminal redundancy; U5, unique 5' sequence; PBS, primer binding site; MA, matrix domain; CA, capsid domain; NC, nucleocapsid domain (extending to the end of Pr74Gag); PR, protease; RT, reverse transcriptase; RH, ribonuclease H; IN, integrase. Location of the primers used for RT-PCR analysis are shown (8). (B) Sequence determined at the breakpoint in the 0.6-kb RT-PCR product; the consensus nucleotides at the splice sites are shown in italic.

S. F. Yu and S. Yendapalli, Division of Basic Sciences, Fred Hutchinson Cancer Research Center, Seattle, WA 98104, USA.
 D. N. Baldwin and M. L. Linial, Division of Basic Sciences, Fred Hutchinson Cancer Research Center, Seattle, WA 98104, and Department of Microbiology, University of Washington, Seattle, WA 98195, USA.
 S. R. Gwynn, Interdisciplinary Program in Molecular and Cellular Biology, and Department of Microbiology, University of Washington, Seattle, WA 98195, USA.

*To whom correspondence should be addressed at the Fred Hutchinson Cancer Research Center.

mRNA is used for Pol translation, we introduced two mutations into the infectious clone that altered the 3'ss upstream of nucleotide 1851 but did not change the reading frame of the Gag protein (Fig. 3A). DNA encoding this 3'ss mutant was transfected into baby hamster kidney (BHK21) cells and viral supernatants were tested in the foamy activation of β -galactosidase (FAB) assay, which measures the ability of a virus to transactivate the HFV LTR (9). The HFV 3'ss mutant clone could not produce infectious virions (Table 1). Results from immunoprecipitations with α -Pol or α -Gag serum show that in wild-type-transfected cells the expected Pol proteins of 125 and 80 kD (4) were detected, whereas no Pol proteins were detected in lysates of cells transfected with the 3'ss mutant (Fig. 3B, left panel). Gag protein could be readily detected in the mutant-transfected cells, indicating similar transfection efficiencies (Fig. 3B, right panel). In wild-type-transfected cells, the 78-kD Gag precursor (Pr78Gag) could be detected as well as the 74-kD cleavage product (P74Gag) (12), which is generated by the virally encoded protease (5). In the mutant-transfected cells, no 74-kD cleavage product was seen. This is expected because protease is included in the precursor Pol protein. In HFV infection, further cleavage of precursor Gag to mature virion proteins is not readily detected. These data show that the splice site

in *gag* is absolutely required for Pol protein synthesis.

We next asked whether the 3'ss mutant could complement two mutants defective in the *gag* gene (GagH1 and GagH3; Fig. 3C). These mutants contain substitutions in the glycine-arginine-rich regions of the nucleocapsid domain and are noninfectious, although they produce both Gag and Pol proteins (13) (Table 1). We found that cotransfection of the 3'ss mutant DNA and either of the Gag mutant DNAs yielded infectious virus (Table 1). The two Gag mutants could not complement each other, demonstrating that we were not detecting DNA recombination. In contrast, in conventional retroviruses, Gag and Pol mutants cannot complement each other because the Gag portion of Gag-Pol cannot substitute for Gag in viral assembly (14). We also created a double stop codon in the *gag* gene 3' of the nucleocapsid domain, in the region cleaved from Pr78Gag. This mutation allows synthesis of P74Gag and a truncated version of P78Gag (Fig. 3C). If a frameshift were required for synthesis of Pol, then this mutation should prevent replication. However, transfection of the GagStop plasmid into cells allowed production of infectious virus (Table 1). Because termination before the normal *gag* UAG in the *pol* overlap region allows viral replication, this result argues against a frameshift mechanism for Gag-Pol synthesis.

There have been no published reports of the structure of the HFV encapsidated genome. We obtained initial data for the presence of DNA as well as RNA in HFV particles using PCR and RT-PCR (13). To analyze more critically the size of this DNA and determine whether it is actually encapsidated within infectious viral particles, we fractionated HFV supernatant particles on a sucrose density gradient and then analyzed fractions for the size of the HFV DNA on a Southern (DNA) blot and for infectivity with the FAB assay. We found a broad peak of infectivity at a density of about 1.14 to 1.18 g/ml (Fig. 4A). DNA of about proviral size [\sim 12 kb as determined from other gels (13)] was also found in this peak when a plus-strand viral-specific probe that would not hybridize to viral RNA was used (Fig. 4B). DNA of this size also hybridized to a minus-strand probe. In preliminary restriction mapping studies, we could not detect any large deletions in the packaged DNA relative to the HFV provirus (13). From separate titration experiments with control plasmid DNA containing full-length HFV, we calculated that there is about one copy of proviral-length DNA per six to nine viral particles (15). Other retroviruses, such as murine leukemia virus and human immunodeficiency virus-type 1, contain some viral DNA, but only 10^{-2} to 10^{-3} copies of short and $\sim 10^{-5}$ copies of full-length DNA are present in virions per RNA molecule, so that DNA can be detected only by PCR (16). HFV contains substantially more proviral length DNA in extracellular virions, indicating that reverse transcriptase of HFV Pol is active in preassembly complexes, in virions before infection of new cells, or both, similar to the reverse transcription pathway of hepadnaviruses. Preliminary experiments with inhibitors of reverse transcriptase indicate

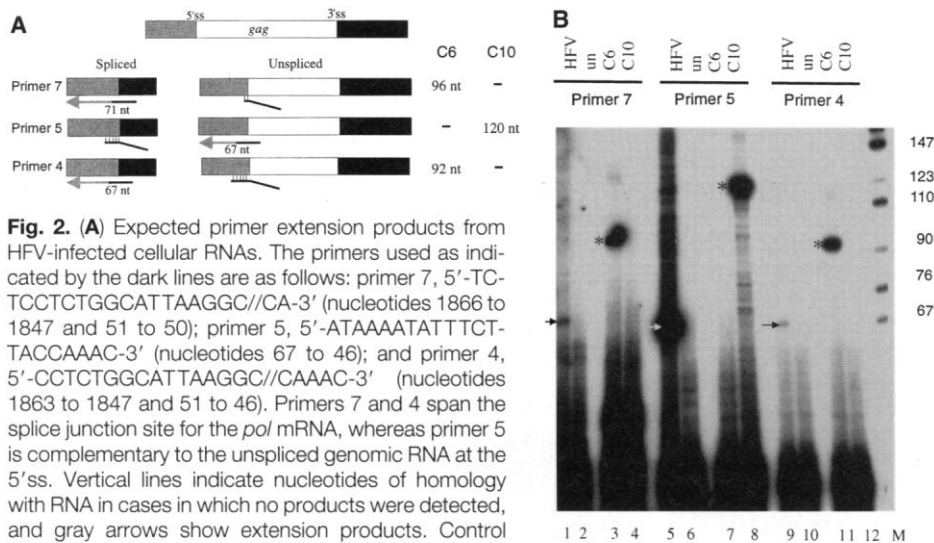


Fig. 2. (A) Expected primer extension products from HFV-infected cellular RNAs. The primers used as indicated by the dark lines are as follows: primer 7, 5'-TCCTCTGGCATTAAGGC//CA-3' (nucleotides 1866 to 1847 and 51 to 50); primer 5, 5'-ATAAAATATTCTTACCAAAC-3' (nucleotides 67 to 46); and primer 4, 5'-CCTCTGGCATTAAGGC//CAAAC-3' (nucleotides 1863 to 1847 and 51 to 46). Primers 7 and 4 span the splice junction site for the *pol* mRNA, whereas primer 5 is complementary to the unspliced genomic RNA at the 5'ss. Vertical lines indicate nucleotides of homology with RNA in cases in which no products were detected, and gray arrows show extension products. Control RNAs were transcribed in vitro from DNA of Bst XI-digested pSGC6 (C6) (spliced control) or Xho I-digested pSGC10 (C10) (unspliced control), with SP6 or T3 polymerase, respectively. Plasmid pSGC6 was generated by deleting a Hind III-Sma I fragment from pSGC5 (8). pSGC10 was constructed by inserting the 361-nucleotide Xba I-Nar I fragment from pHFV13 (-12 to +349) into pBluescriptSKII vector (Stratagene) digested with Xba I and Cla I. The gray and black boxes indicate the exons for *pol* mRNA, and the white box indicates the *gag* intron. **(B)** Results from the primer extension assays. Each lane contained 20 μ g of cellular RNA from uninfected (un) or infected HEL fibroblast cells collected 2 days after infection or 0.2 μ g of control RNA mixed with 3×10^6 cpm of [32 P]oligonucleotide (10 ng). Lane M shows molecular size markers (in kilodaltons) prepared from Msp I-digested pBR322. Black arrows indicate extension products from spliced mRNA and the white arrow indicates those from unspliced genomic RNA. Expected extension products from control RNA are indicated by asterisks.

Table 1. Infectivity after transfection of HFV mutant proviruses. Ten micrograms of each plasmid DNA was used to transfect BHK21 cells. In cases in which two plasmids were cotransfected, 6 μ g of each was used. Two days after transfection, 5 ml of supernatant was collected, filtered, and tested in the FAB assay (9). A negative result indicates that no infectious virions were detected; + indicates a titer of 10^1 to 10^2 infectious units per milliliter; ++ indicates 10^2 to 10^3 per milliliter; and +++ indicates $\geq 10^4$ per milliliter.

| Proviral DNA | Infectivity |
|------------------|-------------|
| Wild type | +++ |
| Pol 3'ss | - |
| GagStop | + |
| GagH1 | - |
| GagH3 | - |
| GagH1 + GagH3 | - |
| Pol 3'ss + GagH1 | ++ |
| Pol 3'ss + GagH3 | ++ |

that additional reverse transcription is required for HFV infectivity. This is consistent with our finding that DNA extracted from virions is not infectious (13).

The data presented here demonstrate that, unlike the conventional retroviruses, expression of HFV Pol requires a spliced mRNA and that reverse transcriptase is activated before release of infectious virions. In many respects, the organization of the HFV genome is similar to other retroviruses, such as the presence of a PBS complementary to tRNA_{1,2}^{lys} at the 5' end of the genome (17) and the order of the major

genes. However, in other retroviruses, Pol is assembled into particles through Gag domains in the Gag-Pol fusion protein (18) and the protease is activated in particles (3), after which a tRNA-Pol complex binds to the primer binding site (19). There are marked similarities between HFV and hepadnaviruses such as hepatitis B virus (HBV). In both, the viral structural (core) protein is not cleaved in virions and its carboxyl end contains stretches of basic amino acids that interact with DNA (13, 20). In HBV, reverse transcriptase (P protein) is translated from genomic-length

RNA by an internal initiation mechanism. Once synthesized, P binds in cis to its own mRNA through a specific region called ϵ , possibly cotranslationally (21). P itself contains a priming domain, and the DNA product is covalently linked to the reverse transcriptase protein (22). Long reverse transcription products appear to require interaction between RNA, P, and the core structural protein in a preassembly complex (23). Genomes found in extracellular HBV particles contain gapped circular DNA molecules rather than RNA. Thus, the bulk of HBV DNA synthesis occurs in a particulate complex and little occurs in the newly infected cells. Both the retroviral and hepadnaviral assembly mechanisms ensure sequestration of active reverse transcriptase in particles and away from cellular mRNAs.

From our data, HFV follows neither paradigm. The mechanism of Pol incorporation into HFV particles is as yet unknown. One possible mechanism for compartmentalization of HFV Pol protein is the presence of domains in the Pol protein that bind with high affinity to Gag domains, leading to rapid encapsidation of Pol into nascent particles. It is also possible that HFV Pol binds with high affinity to the primer binding site region of its genome within cells before encapsidation and binding of the tRNA primer. As for all other known retroviral elements, the foamy virus replication pathway will probably confine reverse transcriptase activity to particle-associated genomes. Foamy viruses share features of the assembly pathway of both retroviruses and hepadnaviruses, but aspects of assembly and reverse transcription are unique to this group. The divergence of HFV from the mode of replication of the other retroviruses, despite great similarities in genome structure, indicates that there is an unexpected plasticity in retroviral replication pathways.

Fig. 3. Viral proteins synthesized by the 3' ss mutant. **(A)** The 3' ss mutant was constructed by a two-step PCR method in which TTA (nucleotides 1844 to 1846) was mutated to CTC (asterisks) without changing the Leu coding sequence. In the first PCR reaction, either combinations of primers MB (5'-TACGCCCGGGAACTGGAGAGCCTCC-3') (nucleotides 1384 to 1398) and SS_{NC}-1 (5'-CTCTGGCATTAAAGGCCGAGAATTCATATACAGCATTTAG-3') (nucleotides 1823 to 1862) or primers SS_{NC}-2 (5'-CTAAATGCTGTATATGAAATCTCGGCCTTAATGCCAGAG-3') (nucleotides 1823 to 1862) and MY (5'-TACGCCCGGGTCCCTTTGATCTCC-3') (nucleotides 2375 to 2389) were used to amplify DNA fragments of 489 or 576 bp from pHFV13. Both fragments were used as templates in the next round of PCR reactions with primers MB and MY, and the resulting fragments were then used to replace wild-type (wt) sequences in the pHFV13 infectious clone. All mutations were confirmed by DNA sequencing. **(B)** Viral proteins in cells transfected with the 3' ss mutant. Control DNA (10 μ g) or plasmid containing proviral DNA from either wild-type (wt) or two clones of the 3' ss mutant was transfected into BHK21 cells with LipofectAmine (Gibco/BRL). Two days after transfection, cells were labeled with [³⁵S]methionine, and cell extracts were immunoprecipitated with rabbit antibody to ribonuclease H (24) (Fig. 2B, left) or antiserum to Gag2 (25) (Fig. 2B, right); un, untransfected BHK21 cells. **(C)** The mutants including GagStop, GagH1, and GagH3 were constructed in a similar manner as the 3' ss mutant. In GagStop, termination codons (TAATAG) were inserted at nucleotide 2297 after the end of the NC domain and in frame with gag coding sequences. The mutation is 31 amino acids before the end of Gag but is not in the Pol open reading frame. In GagH1 and GagH3 the glycine-arginine motif GR box I (nucleotides 1897 to 1930) or GR box II (nucleotides 2082 to 2115) (26) was replaced with an 11-amino acid epitope tag derived from the influenza hemagglutinin protein (27).

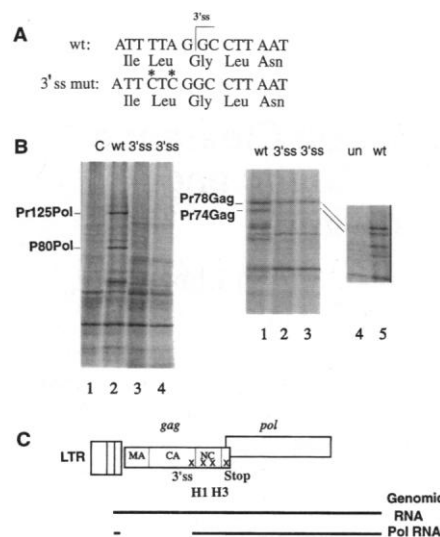
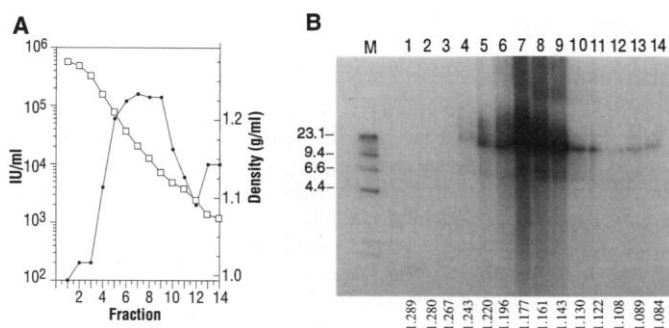


Fig. 4. Sucrose gradient fractionation of HFV extracellular particles. Concentrated (500 \times) HFV virus suspension (0.2 ml) from chronically infected H92.1.7 cells (28) was layered on a 20 to 60% sucrose gradient. Fourteen equal fractions were collected after centrifugation and densities determined. Samples of each fraction were tested with the FAB assay for infectivity (9). The remainder of each fraction was pretreated with deoxyribonuclease I, and nucleic acid was isolated from SDS-lysed virions through use of phenol-chloroform extractions. **(A)** Plot of the infectivity (closed circles) and density (open boxes) of each fraction. **(B)** Southern blot analysis of nucleic acid extracted from each fraction. Nucleic acid was digested with pancreatic ribonuclease A before subjection to Southern blot analysis with a ³²P-labeled plus-strand RNA probe containing HFV sequences from the 5' LTR, gag, and pol. Lane M shows molecular size markers (λ DNA digested with Hind III) in kilobase pairs. The density of each fraction in grams per milliliter is indicated at the bottom.



REFERENCES AND NOTES

1. J. M. Coffin, *Virology*, B. N. Fields and D. M. Knipe, Eds. (Raven, New York, 1990), p. 1437.
2. T. Jacks, *Retroviruses Strategies of Replication*, R. Swanstrom and P. K. Vogt, Eds. (Springer-Verlag, Berlin, 1990), pp. 93-124.
3. S. Oroszlan and R. B. Luftig, in (2), pp. 153-185.
4. K. Netzer *et al.*, *Virology* **192**, 336 (1993).
5. J. Konvalinka, M. Lochelt, H. Zentgraf, R. M. Flügel, H.-G. Kraüsslich, *J. Virol.* **69**, 7264 (1995); M. Lochelt and R. M. Flügel, *ibid.* **70**, 1033 (1996).
6. A. Rethwilm, O. Erlwein, G. Baunach, B. Maurer, V. ter Meulen, *Proc. Natl. Acad. Sci. U.S.A.* **88**, 941 (1991).
7. W. Muranyi and R. M. Flügel, *J. Virol.* **65**, 727 (1991).
8. Total cytoplasmic RNA isolated from uninfected or infected HEL fibroblast cells was subjected to RT-PCR after treatment with deoxyribonuclease I. The first-strand complementary DNA was synthesized by SuperScript II reverse transcriptase (Gibco/BRL) with antisense primer PR2 (5'-CATGGGTACCGTTGCC-CCTGAATCCCAG-3') derived from the 5' region of pol (nucleotides 2405 to 2422; GenBank accession number M19427). Reaction products were subjected to PCR amplification with primers R+3 (5'-GCA-

TCCCGGGGCTCTTCACTACTCGCTCGCT-3') (nucleotides 3 to 23) and PR2, and products were analyzed. A major ~600-bp fragment was isolated from the gel and cloned to generate pSGC5, and the DNA sequence determined.

9. S. F. Yu and M. L. Linal, *J. Virol.* **67**, 6618 (1993).
10. M. Lochelt, H. Zentgraf, R. M. Flügel, *Virology* **184**, 43 (1991).
11. D. N. Baldwin and M. L. Linal, unpublished data.
12. K. O. Netzer, A. Rethwilm, B. Maurer, V. ter Meulen, *J. Gen. Virol.* **71**, 1237 (1990); A. Bartholoma, W. Muranyi, R. M. Flügel, *Virus Res.* **23**, 27 (1992).
13. S. F. Yu and M. L. Linal, unpublished data.
14. K. M. Felsenstein and S. P. Goff, *J. Virol.* **62**, 2179 (1988).
15. Calculation of the number of DNA molecules present in HFV virions was done as follows. An estimated 113 pg of ~12-kb double-stranded DNA was detected from 22 ml of virus supernatant, as determined by Southern blot analysis with pHFV13 plasmid DNA standards. The molecular mass of this ~12-kb double-stranded DNA is about 7.9×10^6 g/mol. Therefore, 113 pg of DNA is equal to 8.9

- $\times 10^6$ DNA molecules. Particle counts determined by electronic microscopy showed that there were about 5.5×10^7 virions present in the 22 ml of viral supernatant. By dividing 8.9×10^6 DNA molecules by 5.5×10^7 virions, we concluded that there is approximately one DNA molecule present in every six virions. In an independent experiment we found a DNA molecule in every nine virions. In viral preparations harvested after 48 hours, we determined that 1 in 25 to 100 supernatant virions is infectious as measured in the FAB assay.
16. F. Lori *et al.*, *J. Virol.* **66**, 5067 (1992); D. Trono, *ibid.*, p. 4893.
17. B. Maurer, H. Bannert, G. Darai, R. M. Flügel, *ibid.* **62**, 1590 (1988).
18. J. W. Wills and R. C. Craven, *AIDS* **5**, 639 (1991).
19. R. Marquet, C. Isel, C. Ehresmann, B. Ehresmann, *Biochimie* **77**, 113 (1995).
20. T. Hatton, S. Zhou, D. N. Standring, *J. Virol.* **66**, 5232 (1992).
21. R. Bartschlagler and H. Schaller, *EMBO J.* **11**, 3413 (1992); R. C. Hirsch, J. E. Lavine, L.-J. Chang, H. E. Varmus, D. Ganem, *Nature* **344**, 552 (1990).
22. G. H. Wang and C. Seeger, *Cell* **71**, 663 (1992); D.

- Ganem, J. R. Pollack, J. Tavis, *Infect. Agents. Dis.* **3**, 85 (1994).
23. M. Nassal and H. Schaller, *Trends. Microbiol.* **1**, 221 (1993).
24. D. Kogel, M. Aboud, R. M. Flügel, *Virology* **213**, 97 (1995).
25. H. Hahn *et al.*, *J. Gen. Virol.* **75**, 2635 (1994).
26. A. W. Schliephake and A. Rethwilm, *J. Virol.* **68**, 4946 (1994).
27. I. A. Wilson *et al.*, *Cell* **37**, 767 (1984).
28. S. F. Yu, J. Stone, M. L. Linal, *J. Virol.* **70**, 1250 (1996).
29. We thank M. Groudine and M. Emerman for their critiques of the manuscript and A. Rethwilm for stimulating discussions about the HFV genome. We also thank A. R. and R. Flügel for providing antisera and L. Caldwell and the electron microscopy facility at the Fred Hutchinson Cancer Research Center for particle counts. Supported by NIH grants CA18282 and HL53762 to M.L.L. S.F.Y. was partially supported by a postdoctoral fellowship (F32 CA60357) from the National Cancer Institute.

26 October 1995; accepted 16 January 1996

HIV-1 Dynamics in Vivo: Virion Clearance Rate, Infected Cell Life-Span, and Viral Generation Time

Alan S. Perelson, Avidan U. Neumann, Martin Markowitz, John M. Leonard, David D. Ho*

A new mathematical model was used to analyze a detailed set of human immunodeficiency virus–type 1 (HIV-1) viral load data collected from five infected individuals after the administration of a potent inhibitor of HIV-1 protease. Productively infected cells were estimated to have, on average, a life-span of 2.2 days (half-life $t_{1/2} = 1.6$ days), and plasma virions were estimated to have a mean life-span of 0.3 days ($t_{1/2} = 0.24$ days). The estimated average total HIV-1 production was 10.3×10^9 virions per day, which is substantially greater than previous minimum estimates. The results also suggest that the minimum duration of the HIV-1 life cycle in vivo is 1.2 days on average, and that the average HIV-1 generation time—defined as the time from release of a virion until it infects another cell and causes the release of a new generation of viral particles—is 2.6 days. These findings on viral dynamics provide not only a kinetic picture of HIV-1 pathogenesis, but also theoretical principles to guide the development of treatment strategies.

HIV-1 replication in vivo occurs continuously at high rates (1, 2). Ho *et al.* (1) found that when a protease inhibitor was administered to infected individuals, plasma concentrations of HIV-1 decreased exponentially, with a mean $t_{1/2}$ of 2.1 ± 0.4 days. Wei *et al.* (2) and Nowak *et al.* (3) found essentially identical kinetics of viral decay after the use of inhibitors of HIV-1 protease or reverse transcriptase. The viral decay observed in these studies was a composite of two separate effects: the clearance of free virions from plasma and the loss of virus-producing cells. To under-

stand the kinetics of these two viral compartments more precisely, we closely monitored the viral load in five HIV-1–infected patients after the administration of a potent protease inhibitor. Using a mathematical model for viral dynamics and nonlinear least squares fitting of the data, we obtained separate estimates of the virion clearance rate, the infected cell life-span, and the average viral generation time in vivo.

Ritonavir (4, 5) was administered orally (600 mg twice daily) to five infected patients, whose base-line characteristics are shown in Table 1. After treatment, we measured HIV-1 RNA concentrations in plasma at frequent intervals (every 2 hours until the sixth hour, every 6 hours until day 2, and every day until day 7) by means of an ultrasensitive modification (1, 5) of the branched DNA assay (6). Each patient responded with a similar pattern of viral de-

cay: an initial lag followed by an approximately exponential decline in plasma viral RNA (see Fig. 1 for examples).

After ritonavir was administered, a delay in its antiviral effect was expected because of the time required for drug absorption, distribution, and penetration into the target cells. This pharmacokinetic delay could be estimated by the time elapsed before the first drop in the titer of infectious HIV-1 in plasma (Table 1 and Fig. 1B). However, even after the pharmacokinetic delay was accounted for, a lag of ~1.25 days was observed before the plasma viral RNA concentration fell (Fig. 1). This additional delay is consistent with the mechanism of action of protease inhibitors, which render newly produced virions noninfectious but do not inhibit either the production of virions from already infected cells or the infection of new cells by previously produced infectious virions (7). In our previous study (1), this additional delay was missed because measurements were less frequent (every 3 days), and the results were fitted to a single exponential, which was sufficient to provide minimum estimates of HIV-1 kinetics. In contrast, in the present study, we obtained 15 data points during the first 7 days, which allowed a careful analysis of the results by means of a new mathematical model of viral kinetics.

We assumed that HIV-1 infects target cells (T) with a rate constant k and causes them to become productively infected cells (T^*). Before drug treatment, the dynamics of cell infection and virion production are represented by

$$\frac{dT^*}{dt} = kVT - \delta T^* \quad (1)$$

$$\frac{dV}{dt} = N\delta T^* - cV \quad (2)$$

A. S. Perelson and A. U. Neumann, Theoretical Division, Los Alamos National Laboratory, Los Alamos, NM 87545, USA.

M. Markowitz and D. D. Ho, Aaron Diamond AIDS Research Center, 455 First Avenue, New York, NY 10016, USA.

J. M. Leonard, Pharmaceutical Products Division, Abbott Laboratories, Abbott Park, IL 60064, USA.

*To whom correspondence should be addressed.